ANTIBIOTIC DISCOVERY

Bioinformatic prospecting and synthesis of a bifunctional lipopeptide antibiotic that evades resistance

Zongqiang Wang[1]†, Bimal Koirala[1]†, Yozen Hernandez[1], Matthew Zimmerman[2], Sean F. Brady[1]*

Emerging resistance to currently used antibiotics is a global public health crisis. Because most of the biosynthetic capacity within the bacterial kingdom has remained silent in previous antibiotic discovery efforts, uncharacterized biosynthetic gene clusters found in bacterial genome–sequencing studies remain an appealing source of antibiotics with distinctive modes of action. Here, we report the discovery of a naturally inspired lipopeptide antibiotic called cilagicin, which we chemically synthesized on the basis of a detailed bioinformatic analysis of the *cil* biosynthetic gene cluster. Cilagicin's ability to sequester two distinct, indispensable undecaprenyl phosphates used in cell wall biosynthesis, together with the absence of detectable resistance in laboratory tests and among multidrug-resistant clinical isolates, makes it an appealing candidate for combating antibiotic-resistant pathogens.

The discovery and therapeutic development of natural product antibiotics, especially those produced by microbes, has substantially reduced mortality caused by bacterial infections (*1*). Unfortunately, this situation is challenged by antibiotic resistance, which is rising at a faster rate than the introduction of molecules with modes of action (MOAs) capable of circumventing existing resistance mechanisms (*2*, *3*). From a clinical development standpoint, nonribosomal peptide synthetase (NRPS)–encoded lipopeptides are an appealing potential source of future antibiotics because they have a history of inhibiting bacterial growth by diverse MOAs (*4*, *5*). Bacterial genome–sequencing efforts have uncovered a large number of biosynthetic gene clusters (BGCs) that do not appear to encode for known natural products, including many that are predicted to encode undescribed lipopeptides. These BGCs likely contain genetic instructions for the biosynthesis of antibiotics with diverse MOAs that could help to replenish antibiotic discovery pipelines. Unfortunately, most sequenced BGCs remain silent in the laboratory, and the molecules they encode remain a mystery. Here, we used a phylogenetic analysis of condensation starter (Cs) domain sequences, which introduce the acyl substituent into lipopeptides, to identify the cryptic *cil* BGC as a potential source of an uncharacterized lipopeptide antibiotic.

To identify BGCs that might encode lipopeptide antibiotics with distinctive MOAs, we collected NRPS BGCs from ~10,000 sequenced bacterial genomes. Clinically relevant lipopeptide antibiotics (e.g., polymyxin, daptomycin, etc.) have historically tended to be larger macrocyclic structures, and therefore BGCs predicted to encode peptides with fewer than five amino acids (i.e., containing fewer than five adenylation domains) were removed from this collection. A recent screen of this collection for BGCs that were predicted to encode congeners of known antibiotics guided our

[1]Laboratory of Genetically Encoded Small Molecules, The Rockefeller University, New York, NY 10065, USA. [2]Center for Discovery and Innovation, Hackensack Meridian Health, Nutley, NJ 07110, USA.
*Corresponding author. Email: sbrady@rockefeller.edu
†These authors contributed equally to this work.

Downloaded from https://www.science.org at Rockefeller University on August 10, 2022

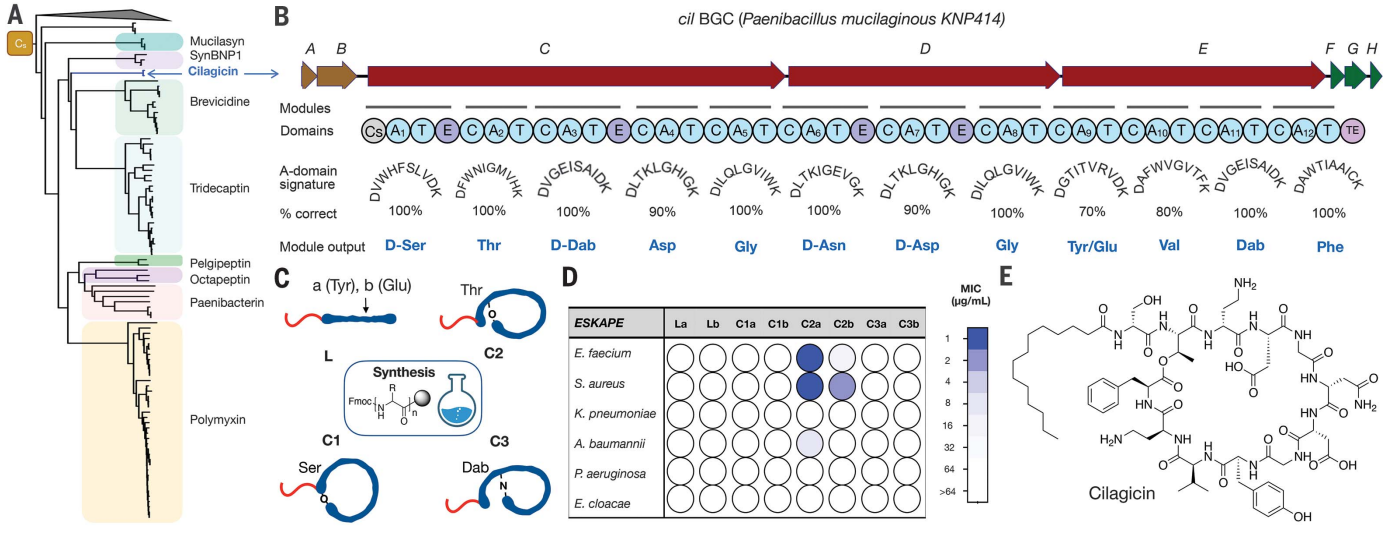

Fig. 1. Discovery of cilagicin. (**A**) Cs domains from sequenced NRPS BGCs were used to construct a phylogenetic tree. Clades associated with characterized antibiotic BGCs are labeled. The "orphan" cilagicin clade is labeled in blue. (**B**) The *cil* BGC contains three NRPS open reading frames (*cil* C to E). Biosynthesis of cilagicin is predicted to start from a Cs domain in CilC and then proceed using one A (adenylation)- and T (thiolation)-domain-containing initiation module, followed by 11 C (condensation)-, A-, and T-domain-containing extender modules. The substrate specificity of the *cil* BGC A domains was predicted on the basis of a comparison of each A domain's substrate-binding pocket against the 10–amino acid A-domain signature sequences found in functional characterized BGCs. E (epimerization) domains in modules 1, 3, 6, and 7 are predicted to result in the incorporation of D amino acids. The thioesterase (TE) domain at the end of *cil* E releases the mature structure from the final T domain as either a linear or cyclic product. (**C**) Diagrams of the four different peptide topologies that were synthesized from the linear peptide predicted to arise from the *cil* BGC. Position 9 was either Tyr (a) or Glu (b). L is a linear peptide. C1, C2, and C3 are cyclized through the C-terminal carboxyl group and Ser-1, Thr-2, or Dab-3, respectively. Dab, 2,4-diaminobutyric acid. (**D**) MIC data against the ESKAPE pathogens for the eight predicted synthetic structures depicted in (C). Concentrations tested ranged from 1 μg/ml (blue) to 64 μg/ml (white). Data are representative of three independent experiments. (**E**) Structure of the antibiotic cilagicin, which corresponds to C2a in (C).

synthesis of macolacin, a colistin analog that is effective against pathogens that express the *mcr-1* resistance gene (*6*). In the current analysis, we searched for uncharacterized BGC families. The key conserved feature across lipopeptides is the presence of an N-terminal lipid that is installed by a Cs domain (*7*–*9*). Among the sequenced large NRPS BGCs that we collected, we identified 3426 that contained a Cs domain. Cs domain sequences from these BGCs were used to construct a phylogenetic tree that guided our discovery efforts. As we have seen with other biosynthetic genes, sequences arising from BGCs sharing close common ancestors, and thus the same MOA, are likely to group together into the same clade (*10*–*12*). By extension, clades that do not contain any sequences from characterized BGCs would represent candidates for identifying structurally and mechanistically new antibiotics. The Cs domain phylogenetic tree contained a number of clades that were not associated with any characterized lipopeptides; however, one was particularly intriguing because it fell into a larger group of sequences in which most other clades were associated with antibiotic biosynthesis. These included BGCs for a number of clinically used, as well as clinically appealing, antibiotics (e.g., polymyxins, tridecaptins, and brevicidines). This "orphan" Cs clade that we identified contained three closely related sequences that arose from the same BGC found in two different sequenced *Paenibacillus mucilaginosus* strains (*KNP414* and *K02*) (Fig. 1A). On the basis of gene content and gene organization, this BGC, which we have called the *cil* BGC, did not resemble any characterized BGCs. Most sequenced BGCs remain silent in the laboratory, even when examined with advanced synthetic biology tools (*13*). With the power of modern synthetic organic chemistry and the increasing accuracy of natural product structure prediction algorithms, it is now possible to generate a bioactive molecule from the genetic instructions found in the primary sequence of a BGC. This was done by first bioinformatically predicting the encoded structure and then chemically synthesizing the predicted structure, i.e., producing a synthetic-bioinformatic natural product, syn-BNP (*14*–*16*). In this study, we used a syn-BNP approach to generate lipopeptide structures on the basis of the *cil* BGC and then tested these small molecules for antibacterial activity.

The *cil* BGC contains three NRPS open reading frames (*cil* C to E) that encode 12 distinct modules (Fig. 1B and table S1). The biosynthesis of a 12-mer lipopeptide is predicted to begin with the Cs domain at the N terminus of CilC and end with the thioesterase at the C terminus of CilE. The composition of each module's A-domain substrate-binding pocket (i.e., the substrate signature based on positions 235, 236, 239, 278, 299, 301, 322, 330, 331, and 517 of the A domain) was used to predict the 12 monomers used by this BGC (*17*). Eleven A domains had perfect or near perfect (80%) matches to characterized A domains, so we could make high-confidence predictions for the amino acid incorporated by these modules. The A-domain substrate signature from module 9 had equally good matches (70%) to two amino acids, Tyr and Glu. This analysis gave us two potential predicted linear lipopeptide products for the *cil* BGC: La and Lb (Fig. 1C). Epimerization domains found in modules 1, 3, 6, and 7 indicated that these amino acids appear in the D configuration in the *cil* BGC product. The absence of any genes predicted to encode tailoring enzymes (i.e., methyltransferase, hydroxylation, amino transferase, glycosyl transferase, etc.) within 10 kB of the *cil* NRPS genes suggested that the product of the *cil* BGC was not modified beyond the NRPS-produced lipopeptide (*18*).

Naturally occurring lipopeptides appear as either linear or cyclic structures. The predicted *cil* linear peptide contains three amino acids, D-Ser-1, Thr-2, and D-Dab-3, that could serve as nucleophiles for cyclization through the C-terminal carboxyl. Bringing together our linear peptide prediction and three potential cyclization sites yielded eight structures (two linear and six cyclic) that we predicted could arise from the *cil* BGC (Fig. 1C). Each of the eight potential BGC products was generated by solid-phase peptide synthesis (table S2). The *cil* BGC does not contain any lipid biosynthetic genes, so we predicted that the lipid found on the product of the *cil* BGC would arise directly from native fatty acid biosynthesis. Among the characterized bacterial lipopeptides, myristic acid is one of the most frequently seen simple lipids, so all synthetic peptides were N-terminal acylated with myristic acid.

All eight synthetic structures were assayed for activity against the ESKAPE pathogens (*Enterococcus faecium*, *Staphylococcus aureus*, *Klebsiella pneumoniae*, *Acinetobacter baumannii*, *Pseudomonas aeruginosa*, and *Enterobacter* species) (Fig. 1D and table S3). The 11–amino acid macrocycle that was cyclized through the hydroxyl of Thr-2 and contained Tyr at position 9 (compound C2a) showed potent antibacterial activity against the two Gram-positive ESKAPE pathogens [minimum inhibitory concentration (MIC), 1 μg/ml]. None of the remaining close analogs that we synthesized showed more potent activity against

Table 1. Activity of cilagicin against microorganisms and human cells.

Pathogens/human cells	Cilagicin MIC (μg/ml)*
Gram-positive	
Staphylococcus aureus USA300 (MRSA)	1
Staphylococcus aureus BAA1717(BRSA)	0.5
Enterococcus faecium EF18 (VRE)	0.5
Enterococcus faecalis AR785 (VRE)	0.5
Enterococcus gallinarum AR784 (VRE)	0.5
Enterococcus casseliflavus AR798 (VRE)	0.125
Streptococcus pneumoniae R†	0.5
Streptococcus pneumoniae Tigr4†	0.25
Clostridium difficile HM89‡	2
Clostridium difficile HM746‡	2
Streptococcus pyrogens ATCC19615	0.125
Streptococcus agalactiae BAA2675	1
Streptococcus agalactiae BAA1176	1
Bacillus subtilis 168A1	2
Gram-negative	
Acinetobacter baumannii ATCC17978	8
Escherichia coli BAS849	4
Escherichia coli ATCC25922	>64
Klebsiella pneumoniae ATCC13833	>64
Pseudomonas aeruginosa PAO1	>64
Enterobacter cloacae ATCC13047	>64
Human cell line	
HEK293	>64‡

*The MIC was tested by broth microdilution. †Bacteria were cultured under 5% CO_2. ‡Bacteria were cultured under anaerobic conditions. MRSA, methicillin-resistant *S. aureus*; BRSA, bacitracin-resistant *S. aureus*; VRE, vancomycin-resistant Enterococci.

Downloaded from https://www.science.org at Rockefeller University on August 10, 2022

these strains. We have called the active structure cilagicin (Fig. 1E).

Cilagicin was active against all Gram-positive pathogens that we tested (Table 1). It was also active against a number of difficult-to-treat vancomycin-resistant *Enterococci* pathogens, as well as *Clostridioides difficile*, both of which are considered urgent and serious threat pathogens by the US Centers for Disease Control and Prevention (CDC) (*19*). It was also active against all antibiotic-resistant Gram-positive pathogens that we tested. It maintained potent activity against a panel of 19 *S. aureus* strains that showed different patterns of resistance to clinically relevant families of antibiotics (table S4). Further, in stark contrast to US Food and Drug Administration (FDA)–approved antibiotics, cilagicin maintained potent activity against all strains found in a panel of 30 vancomycin-resistant *Enterocci* clinical isolates (table S5). This collection is highly enriched in multidrug-resistant (MDR) isolates, with more than half exhibiting resistance to between five and eight different clinically used antibiotics. Cilagicin was largely inactive against Gram-negative bacteria, with the exception of *A. baumannii* (table S6) and outer membrane–permeabilized *Escherichia coli* BAS849, suggesting that the outer membrane of Gram-negative bacteria blocks cilagicin's access to its target. Even at the highest concentration we tested, cilagicin did not show human cell line cytotoxicity (Table 1).

In a time-dependent killing curve analysis, cilagicin was found to be bactericidal and to reduce the number of viable bacteria by more than four orders of magnitude after 4 hours (Fig. 2A). Electron microscopy images of cilagicin-treated cells showed cell collapse over time (Fig. 2B). In an effort to elucidate cilagicin's MOA, we tried to raise mutants by direct plating of *S. aureus* on cilagicin. In these direct plating experiments, we never observed any colonies that showed more than a onefold increase in MIC. To explore the possibility of cilagicin having a detergent-like activity, we tested it for membrane depolarization and cell lytic activities using 3,3′-dipropylthiadicarboncyanine iodide [$DiSC_3(5)$]– and SYTOX–based fluorescence assays, respectively (Fig. 2, C and D) (*20*–*22*). No response was detected in either assay when *S. aureus* was exposed to even eightfold the MIC of cilagicin, ruling out membrane disruption as its MOA.

Cilagicin is a zwitterion with two positively charged residues, 3-D-Dab and 11-D-Dab, and two negatively charged residues, 4-Asp and 7-D-Asp. Charged lipopeptide antibiotics often do not enter the cell and instead function by disrupting synthesis of the cell wall outside the cell membrane (*11*, *23*, *24*). Antibiotics that block peptidoglycan biosynthesis lead to the accumulation of the lipid II precursor UDP-MurNAc-pentapeptide, which is easily detected by liquid chromatography–mass spectroscopy (LC-MS) in antibiotic-exposed cultures (*11*, *25*–*27*). LC-MS analysis of *S. aureus* cultures exposed to cilagicin (1× MIC) showed an obvious accumulation of UDP-MurNAc-pentapeptide (Fig. 2E). Because it is often much more difficult to alter a small-molecule target than a protein target through genomic mutations, our inability to identify cilagicin-resistant mutants hinted at the binding of a small molecule instead of a protein as the mode of inhibiting cell wall biosynthesis. To identify the

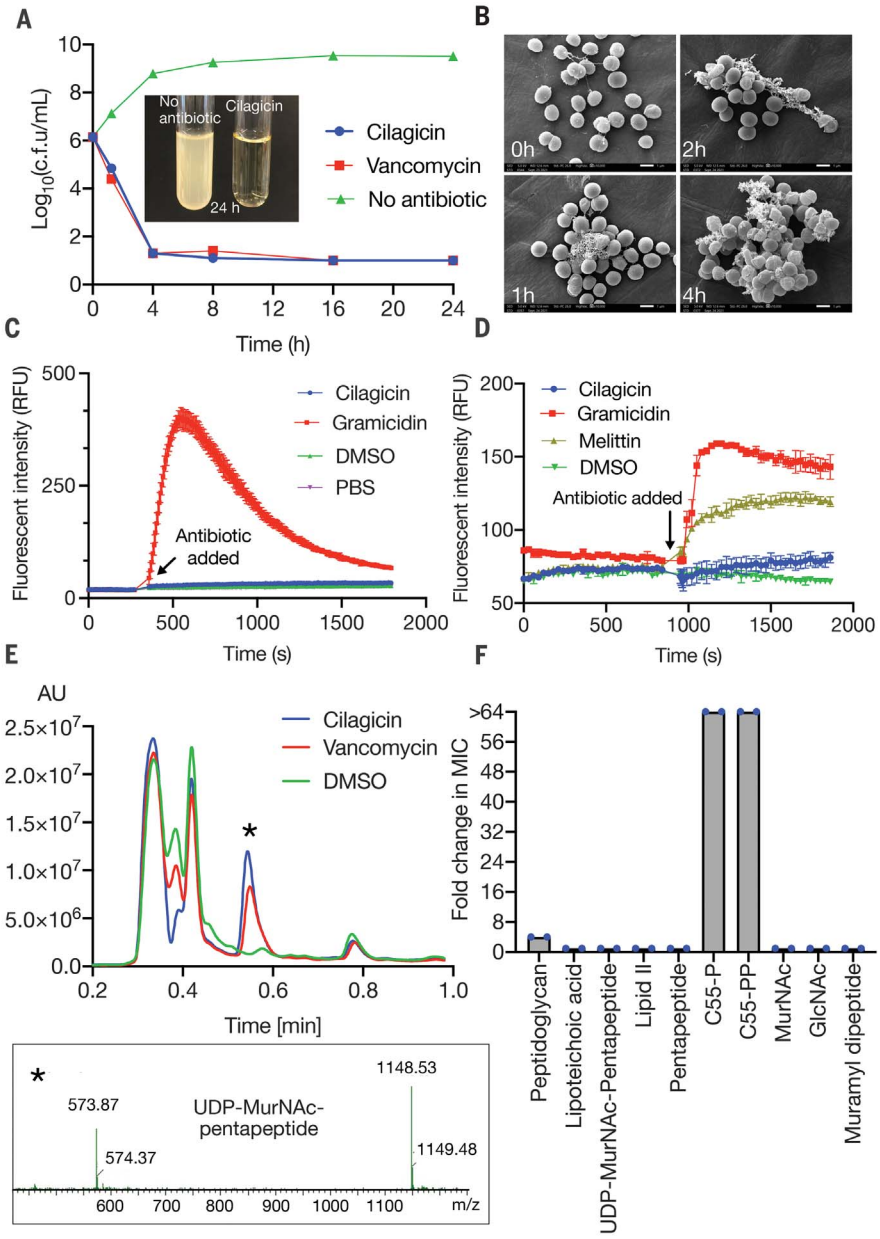

Fig. 2. Cilagicin mode of action. (**A**) Survival of *S. aureus* USA300 after timed exposure to 10× the MIC of cilagicin. Dimethyl sulfoxide (DMSO) and vancomycin (10× MIC) were included as controls. CFUs were counted three independent times and are plotted as mean ± SD. (**B**) Scanning electron microscopy image of *S. aureus* USA300 cultures treated with cilagicin. Conditions were the same as in (A). (**C** and **D**) Cell lysis (C) or membrane depolarization (D) in cilagicin-treated *S. aureus* cultures was monitored using SYTOX and DiSC3(5) dyes, respectively. Data are presented as the mean of three independent experiments ± SD. (**E**) Accumulation of UDP-MurNAc-pentapeptide after treating *S. aureus* cultures with cilagicin (1× MIC) was monitored by LC-MS. DMSO- and vancomycin (10× MIC)–treated cultures were examined as controls. UDP-MurNAc-pentapeptide corresponds to $[M\text{-}H]^-$ = 1148.53 and $[M\text{-}2H]^{2-}$ = 573.87. (**F**) Fold change in cilagicin MIC upon treatment of *S. aureus* with fivefold molar excess of different lipid II intermediates. The peptidoglycan mixture was added at 100 μg/ml. Data are representative of two independent experiments.

Downloaded from https://www.science.org at Rockefeller University on August 10, 2022

metabolite(s) that interacts with cilagicin, we screened a series of lipid II intermediates for their ability to suppress cilagicin's antibacterial activity (Fig. 2F). In these studies, the MIC of cilagicin against *S. aureus* USA300 was determined in the presence of a fivefold molar excess of each metabolite. Two of the compounds that we tested, undecaprenyl phosphate (C55-P) and undecaprenyl pyrophosphate (C55-PP), showed dose-dependent inhibition of cilagicin's antibacterial activity (Fig. 3, A and B).

C55-P is a monophosphorylated, 55-carbon-long isoprene that is essential for transporting intermediates in the biosynthesis of cell wall carbohydrate polymers (e.g., peptidoglycan, O antigen, teichoic acids, etc.) across the bacteria cell membrane (*28*, *29*). C55-PP is the diphosphorylated version of the same 55-carbon isoprene. It is both produced de novo and recycled from C55-P during the biosynthesis of the cell wall. Its dephosphorylation by membrane-embedded pyrophosphatases generate the cellular pool of C55-P that is required for cell wall synthesis (*30*). Using isothermal titration calorimetry, we observed that cilagicin bound both C55-P and C55-PP (Fig. 3, C and D), but a representative inactive analog from our initial synthesis studies, cilagicin-3b, did not bind either compound. Collectively, our MOA studies are consistent with cilagicin being able to sequester both C55-P and C55-PP and thus acting as a bifunctional antimicrobial.

Bacteria only have a small pool of free undecaprenyl carrier lipids (~10^5 molecules per cell) to use in the transfer of critical biosynthetic intermediates across the cell membrane (*31*). Although disruption of this process is an appealing antibacterial MOA, it remains underexploited clinically because only a few antibiotics have been identified that bind even one undecaprenyl phosphate. These include the antibiotics bacitracin and tripropeptin, which specifically bind C55-PP in a zinc- and calcium-dependent manner, respectively (*32*, *33*). The only known antibiotics that bind C55-P are the calcium-dependent lipopeptide friulimicin and its close congeners (e.g., amphomycin and laspartomycin) (*26*, *27*, *34*). Binding C55-P directly reduces the amount of available C55-P, whereas sequestering C55-PP indirectly reduces C55-P by preventing C55-PP dephosphorylation. In either case, this disrupts the flow of peptidoglycan precursors into the cell wall, ultimately leading to cell death (Fig. 3E).

Bacitracin is used clinically as a topical antibiotic, and friulimicin is in development for use in animal health. Unfortunately, bacteria exposed to antibiotics that bind a single undecaprenyl phosphate are reported to readily develop resistance. Antibiotics with multiple molecular targets tend to have reduced rates of resistance because of the difficulty associated with altering multiple targets simultaneously. Therefore, we predicted that in

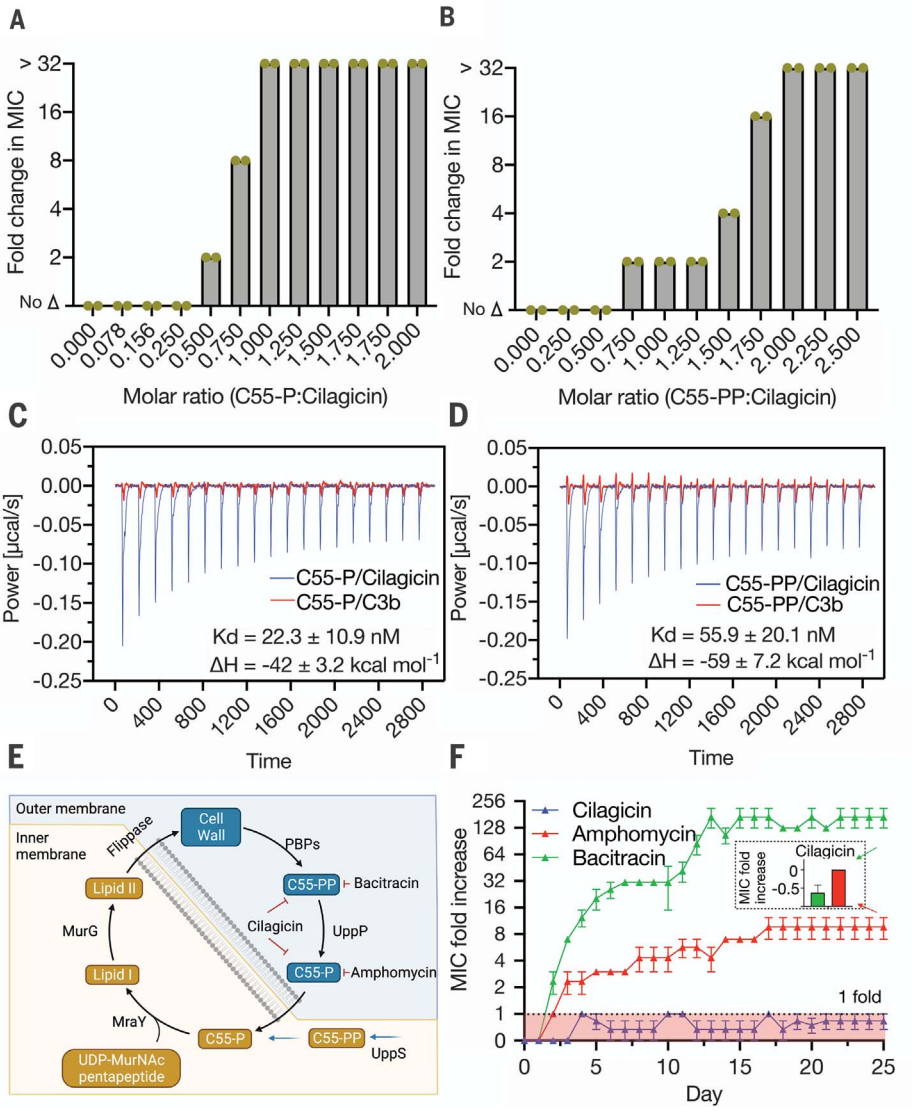

Fig. 3. Interaction of cilagicin with C55-P and C55-PP. (**A** and **B**) Fold change in MIC of cilagicin-treated cultures of *S. aureus* USA300 in the presence of different concentrations of C55-P (A) or C55-PP (B). The highest concentration tested was 32× the MIC. Data from two independent experiments are presented. (**C** and **D**) Isothermal titration calorimetry data for cilagicin or its inactive analog C3b interacting with either C55-P (C) or C55-PP (D). Two independent experiments were performed with similar results. (**E**) Diagram of the role of C55-P and C55-PP in Gram-positive cell wall biosynthesis. (**F**) Resistance acquisition during serial passaging of *S. aureus* USA300 in the presence of sub-MIC levels of cilagicin, bacitracin, or amphomycin. Data shown represent the mean of three independent experiments ± SEM. Inset: Fold increase in the MIC of cilagicin against bacitracin (green)– and amphomycin (red)–resistant strains at 25 days.

the case of cilagicin, its ability to bind both undecaprenyl phosphates (i.e., two distinct small molecules) would lead to a reduced resistance rate compared with antibiotics that bind a single phosphorylated undecaprenyl moiety. Because we had failed to identify mutants resistant to cilagicin by direct plating on antibiotic-containing media, we attempted to raise *S. aureus*–resistant mutants by daily serial passage in the presence of sub-MIC levels of antibiotic using cilagicin, bacitracin, or the friulimicin congener amphomycin to allow a direct comparison of resistance rates for antibiotics that bind either one or two phosphorylated undecaprenyl moieties. *S. aureus* rapidly developed resistance to both bacitracin and amphomycin. MICs for these antibiotics increased by eightfold to 256-fold, respectively, during the course of the serial passage experiment. By contrast, after 25 days of constant exposure to cilagicin, we observed no higher than a doubling of the original MIC (Fig. 3F). In addition, neither the highly bacitracin-resistant mutants nor the highly amphomycin-resistant mutants that we generated showed cross-resistance to cilagicin. The *cil* BGC is found in the genome of

Downloaded from https://www.science.org at Rockefeller University on August 10, 2022

A

Lipid substituent		MIC	Fold increase
Cila	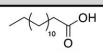	1	32
L1	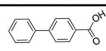	4	0
L2	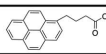	0.5	16
L3	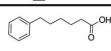	8	0
L4		8	1
L5	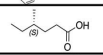	4	0
L6	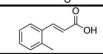	64	0

B

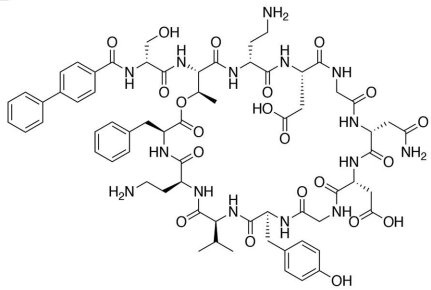

Cilagicin BP

C

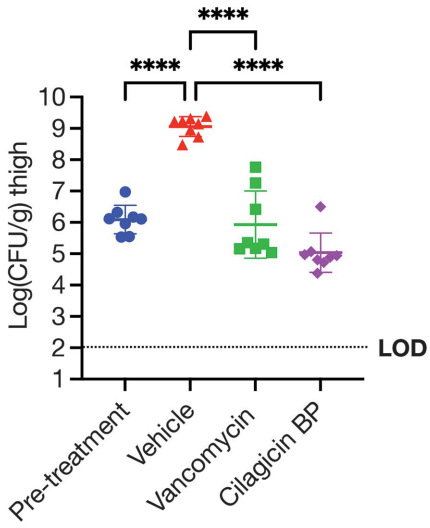

D

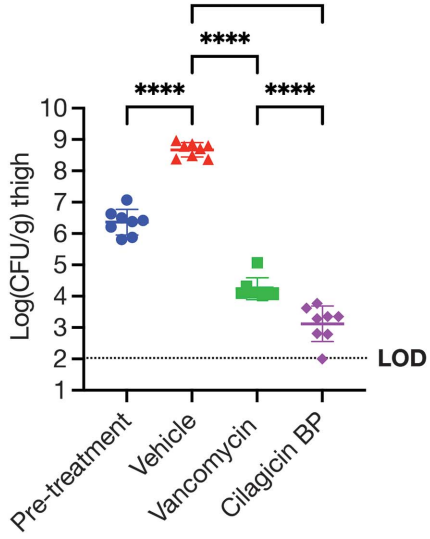

Fig. 4. Cilagicin BP activity in a murine neutropenic thigh infection model. (**A**) Anti–*S. aureus* activity of cilagicin analogs with different lipid substituents in the presence of 10% serum. Blue indicates MIC <4 μg/ml or no change in MIC in the presence of serum. (**B**) Structure of cilagicin BP (L1). (**C**) Neutropenic thigh infection model using *S. aureus* USA300. (**D**) Neutropenic thigh infection model using *S. pyrogens* ATCC19615. Two hours after infection with a fresh bacterial suspension (1×10^6 CFUs), vehicle (10% DMSO, TID), vancomycin (40 mg/kg, TID), or cilagicin BP (40 mg/kg, TID) was delivered by intraperitoneal injection. Twenty-four hours after infection, CFUs were determined from homogenized thigh tissue samples. Significant differences between groups were analyzed by one-way analysis of variance (ANOVA) (***P = 0.0001, ****P < 0.0001) (n = 4 mice, n = 8 thighs). Mean CFU counts and SDs are shown.

P. mucilaginosus. The genus *Paenibacillus* is Gram variable. *P. mucilaginosus*'s reported negative Gram staining suggests that it contains an outer membrane that could protect it from cilagicin's toxicity, thus potentially eliminating the need for self-resistance elements to have evolved in nature (*35*, *36*).

Bacitracin resistance arises from the release of C55-PP from bacitracin by the ABC transporter BceAB, increased production of C55-PP by the undecaprenyl-pyrophosphate phosphatase BcrC, or by a still ill-defined mechanism associated with phage shock protein–like protein expression (LiaI and LiaH) (*37*). In the case of C55-P binding, antibiotic resistance is associated with the expression of the cell envelope stress response regulator (*38*), which provides only low-level resistance compared with what is seen for bacitracin-resistance mechanisms (less than eightfold versus more than 254-fold MIC increases, respectively). Because the binding of C55-P alone appears to be difficult to overcome, it was not surprising that sequestration of the entire pool of undecaprenyl phosphates by cilagicin would further reduce the propensity for resistance to develop. In general, the sequestration of an essential extracellular metabolite is an appealing MOA because the development of resistance has often proved difficult in laboratory experiments using individual pathogens (*39*). Historically, once these antibiotics are exposed to the global pool of resistance determinants present in the clinical setting, resistance might appear, albeit often at a much slower rate than is seen for other MOAs. Although we have not yet observed cilagicin resistance in MDR clinical isolates, this does not rule out the eventual appearance of resistance with broader environmental exposure.

Our initial pharmacological assessment in mice showed that cilagicin had high plasma bioavailability when delivered by intraperitoneal injection (Fig. S2). However, it did not reduce bacterial burden in an animal infection model. We subsequently observed that cilagicin's antibacterial activity was significantly suppressed in the presence of serum, suggesting that high serum binding might have also limited its in vivo activity (Fig. 4A). We therefore attempted to generate a cilagicin analog with reduced serum binding. To do this, we created a collection of cilagicin analogs with different N-terminal lipids and compared their MICs in the presence and absence of serum. An analog containing a biphenyl N-terminal substituent, cilagicin BP, maintained good antimicrobial activity and showed no increase in MIC in the presence of serum (Fig. 4B and table S7). Similar biphenyl substituents are found in several synthetically optimized natural product antibiotics, including glycopeptides (oritavancin) and other lipopeptides (macolacin) (*6*, *40*). This change of lipid substituent did not alter the antibiotics' MOA (Fig. S3A), and cilagicin BP continued to show no hemolytic activity and no human cell cytotoxicity (Fig. S3, B and C). We assessed the in vivo efficacy of cilagicin BP using a neutropenic mouse thigh model. At 24 hours after infection, cilagicin BP showed significant antibacterial activity against *S. aureus* USA300 at 40 mg/kg given three times a day (TID), resulting in an almost 4 $\log_{10}$ reduction in colony-forming units (CFUs) compared with the vehicle control (Fig. 4C). Next, we evaluated cilagicin BP against *S. pyrogens* ATCC19615 in the same neutropenic thigh model. In this case, cilagicin BP showed an even more impressive reduction (>5 $\log_{10}$) in bacterial burden compared with the vehicle control, which was consistent with the lower MIC values for this pathogen in vitro (Fig. 4D). Cilagicin BP resulted in more than a log greater reduction of bacterial burden than vancomycin against *S. pyrogens*.

Cilagicin BP's mode of action, absence of detectable resistance, and in vivo activity make it an appealing lead structure for the development of a next-generation antibiotic that may help to address the growing antibiotic resistance crisis. As seen with the characterization of biologically produced natural products, the

Downloaded from https://www.science.org at Rockefeller University on August 10, 2022

study of syn-BNPs that are inspired by unexplored BGC families should prove to be a productive strategy for identifying distinctive scaffolds that can serve as lead structures for developing antibiotics with diverse MOAs.

REFERENCES AND NOTES

1. S. E. Rossiter, M. H. Fletcher, W. M. Wuest, *Chem. Rev.* **117**, 12415–12474 (2017).
2. J. Davies, D. Davies, *Microbiol. Mol. Biol. Rev.* **74**, 417–433 (2010).
3. B. Aslam *et al*., *Infect. Drug Resist.* **11**, 1645–1658 (2018).
4. I. W. Hamley, *Chem. Commun.* **51**, 8574–8583 (2015).
5. J. M. Raaijmakers, I. De Bruijn, O. Nybroe, M. Ongena, *FEMS Microbiol. Rev.* **34**, 1037–1062 (2010).
6. Z. Wang *et al*., *Nature* **601**, 606–611 (2022).
7. K. Bloudoff, T. M. Schmeing, *Biochim. Biophys. Acta. Proteins Proteomics* **1865** (11 Pt B), 1587–1604 (2017).
8. C. Rausch, I. Hoof, T. Weber, W. Wohlleben, D. H. Huson, *BMC Evol. Biol.* **7**, 78 (2007).
9. N. Roongsawang *et al*., *FEMS Microbiol. Lett.* **252**, 143–151 (2005).
10. H. S. Kang, S. F. Brady, *ACS Chem. Biol.* **9**, 1267–1272 (2014).
11. B. M. Hover *et al*., *Nat. Microbiol.* **3**, 415–422 (2018).
12. Z. Wang *et al*., *Angew. Chem.* **133**, 22346–22351 (2021).
13. H. A. Tomm, L. Ucciferri, A. C. Ross, *J. Ind. Microbiol. Biotechnol.* **46**, 1381–1400 (2019).
14. J. Chu *et al*., *Nat. Chem. Biol.* **12**, 1004–1006 (2016).
15. J. Chu *et al*., *J. Am. Chem. Soc.* **142**, 14158–14168 (2020).
16. J. Chu, X. Vila-Farres, S. F. Brady, *J. Am. Chem. Soc.* **141**, 15737–15741 (2019).
17. T. Stachelhaus, H. D. Mootz, M. A. Marahiel, *Chem. Biol.* **6**, 493–505 (1999).
18. C. T. Walsh *et al*., *Curr. Opin. Chem. Biol.* **5**, 525–534 (2001).
19. Centers for Disease Control and Prevention, "Antibiotic resistance threats in the United States 2019" (CDC, 2019); https://www.cdc.gov/drugresistance/pdf/threats-report/2019-ar-threats-report-508.pdf.
20. B. L. Roth, M. Poot, S. T. Yue, P. J. Millard, *Appl. Environ. Microbiol.* **63**, 2421–2431 (1997).
21. G. Cabrini, A. S. Verkman, *J. Membr. Biol.* **92**, 171–182 (1986).
22. M. Wu, E. Maier, R. Benz, R. E. Hancock, *Biochemistry* **38**, 7235–7242 (1999).
23. C. Wu, Z. Shang, C. Lemetre, M. A. Ternei, S. F. Brady, *J. Am. Chem. Soc.* **141**, 3910–3919 (2019).
24. S. A. Cochrane *et al*., *Proc. Natl. Acad. Sci. U.S.A.* **113**, 11561–11566 (2016).
25. L. L. Ling *et al*., *Nature* **517**, 455–459 (2015).
26. T. Schneider *et al*., *Antimicrob. Agents Chemother.* **53**, 1610–1618 (2009).
27. L. H. Kleijn *et al*., *J. Med. Chem.* **59**, 3569–3574 (2016).
28. T. Touzé, D. Mengin-Lecreulx, *Ecosal Plus* **3**, 10.1128/ecosalplus.4.7.1.7 (2008).
29. J. van Heijenoort, *Nat. Prod. Rep.* **18**, 503–519 (2001).
30. M. El Ghachi *et al*., *Nat. Commun.* **9**, 1078 (2018).
31. V. M. Hernández-Rocamora *et al*., *Cell Surf.* **2**, 1–13 (2018).
32. H. Hashizume *et al*., *Antimicrob. Agents Chemother.* **55**, 3821–3828 (2011).
33. K. J. Stone, J. L. Strominger, *Proc. Natl. Acad. Sci. U.S.A.* **68**, 3223–3227 (1971).
34. M. Singh, J. Chang, L. Coffman, S. J. Kim, *Sci. Rep.* **6**, 31757 (2016).
35. X. F. Hu *et al*., *Int. J. Syst. Evol. Microbiol.* **60**, 8–14 (2010).
36. D. Goswami, S. Parmar, H. Vaghela, P. Dhandhukia, J. N. Thakker, *Cogent Food Agric.* **1**, 1000714 (2015).
37. J. Radeck *et al*., *Mol. Microbiol.* **100**, 607–620 (2016).
38. T. Wecke *et al*., *Antimicrob. Agents Chemother.* **53**, 1619–1623 (2009).
39. D. G. J. Larsson, C. F. Flach, *Nat. Rev. Microbiol.* **20**, 257–269 (2021).
40. K. D. Brade, J. M. Rybak, M. J. Rybak, *Infect. Dis. Ther.* **5**, 1–15 (2016).
41. Z. Wang, B. Koirala, Y. Hernandez, M. Zimmerman, S. F. Brady, Code for: Bioinformatic prospecting and synthesis of a bifunctional lipopeptide antibiotic that evades resistance, Zenodo (2022); https://doi.org/10.5281/zenodo.5793911.

ACKNOWLEDGMENTS

We thank J. C. Vederas for providing synthetic lipid II(lys), the CDC for providing vancomycin-resistant strains, the Rockefeller University High Throughput Screening and Spectroscopy Resource Center for assistance with isothermal titration calorimetry experiments, the Rockefeller University Comparative Bioscience Center for help with animal studies, and the Rockefeller University Electron Microscopy Resource Center for collecting scanning electron microscope data. **Funding:** This work was supported by the National Institutes of Health (grants 1U19AI142731 and 5R35GM122559). **Author contributions:** S.F.B. and Z.W. designed the study and analyzed the data. Z.W. performed the biochemical experiments. B.K. performed the peptide synthesis. Z.W. and Y.H. performed the bioinformatic analysis. M.Z. performed the pharmacokinetics assay. S.F.B. and Z.W. designed the animal study. S.F.B. and Z.W. prepared the manuscript. All authors were involved in discussing the results and reviewing the manuscript. **Competing interests:** A patent covering the structure and activity of cilagicin has been filed by Rockefeller University. S.F.B. consulted for Lodo Therapeutics and Zymergen and has Zymergen stock options. The remaining authors declare no competing interests. **Data and materials availability:** The genome sequences of *P. mucilaginosus* K02 and KNP414 are available in GenBank under accession numbers NC_017672.3 and NC_015690.1, respectively. BGCs were collected from antiSMASH-db (version 2.0). The Perl script used to identify lipopeptide BGCs can be accessed through Zenodo (*41*). NMR spectra for cilagicin and cilagicin BP are presented in the supplementary materials. All data are available in the main text or the supplementary materials. **License information:** Copyright © 2022 the authors, some rights reserved; exclusive licensee American Association for the Advancement of Science. No claim to original US government works. https://www.science.org/about/science-licenses-journal-article-reuse

SUPPLEMENTARY MATERIALS

science.org/doi/10.1126/science.abn4213
Materials and Methods
Figs. S1 to S9
Tables S1 to S7
References (*42*–*45*)
MDAR Reproducibility Checklist

View/request a protocol for this paper from *Bio-protocol*.

Submitted 29 November 2021; accepted 6 April 2022
10.1126/science.abn4213

Downloaded from https://www.science.org at Rockefeller University on August 10, 2022

Science

Bioinformatic prospecting and synthesis of a bifunctional lipopeptide antibiotic that evades resistance

Zongqiang WangBimal KoiralaYozen HernandezMatthew ZimmermanSean F. Brady

Science, 376 (6596), • DOI: 10.1126/science.abn4213

Panning for antibiotics that stand out

Despite their importance in modern medicine, antibiotics are under constant threat as pathogens adapt, acquire, or evolve resistance with chilling regularity. Finding new molecules and mechanisms is one way that we can keep ahead. Panning genomes enriched in secondary metabolites, Wang *et al*. used a computational approach to predict the structure of a cyclic nonribosomal lipopeptide antibiotic, which they named “cilagicin” (see the Perspective by Seipke). Chemical synthesis of the predicted peptide revealed potent and broad antimicrobial activity against Gram-positive bacteria, including a number of drug-resistant pathogens, and a cilagicin derivative protected mice in an acute infection model. Mechanistic experiments suggested the peptide binds to two closely related molecules involved in lipid biosynthesis, an ability that may help to prevent the rapid development of resistance. —MAF

View the article online
https://www.science.org/doi/10.1126/science.abn4213
Permissions
https://www.science.org/help/reprints-and-permissions

Downloaded from https://www.science.org at Rockefeller University on August 10, 2022

Use of this article is subject to the Terms of service

Science (ISSN) is published by the American Association for the Advancement of Science. 1200 New York Avenue NW, Washington, DC 20005. The title *Science* is a registered trademark of AAAS.
Copyright © 2022 The Authors, some rights reserved; exclusive licensee American Association for the Advancement of Science. No claim to original U.S. Government Works